JOURNAL OF MATERIALS SCIENCE 18 (1983) 3249–3258

Plastic deformation and dislocation structure of single crystal mercuric iodide*

TIMOTHY W. JAMES,† FREDERICK MILSTEIN
Department of Mechanical and Environmental Engineering, University of California, Santa Barbara, CA 93106, USA

A systematic investigation of plasticity in single crystal mercuric iodide was carried out. Over eighty compression tests were performed on single crystal specimens oriented variously with respect to the axis of loading. Three characteristic loading responses were observed and classified according to crystal orientation, as follows: (a) the direction of load was perpendicular to the [0 0 1] axis, (b) the loading direction was parallel to [0 0 1] and (c) the load was neither parallel nor perpendicular to [0 0 1]. In cases a and b, under sufficient load, the samples always exhibited brittle failure (without prior plastic deformation) whereas, in case c, the samples were always easily plastically deformed by slip of (0 0 1) planes. The case c plastic deformation also exhibited work hardening. A dislocation model for plasticity in mercuric iodide is induced from the experimental results. The model consists of "easy glide" dislocations, the cores of which are parallel to (0 0 1) planes, and "hard glide" dislocations that intersect the (0 0 1) planes. Movement of the easy glide dislocations causes the (0 0 1) slip in case c, whereas interactions between the easy and hard glide dislocations account for the work hardening. The results of other experiments (including creep, annealing, microscopic observation of dislocation etch pits, and bending) are consistent with the model. Deformation during large angle bending tests is a particularly remarkable phenomenon.

1. Introduction

The present paper (i) reports the results of what evidently has been the first systematic investigation of plasticity in single crystal mercuric iodide (HgI_2) and (ii) presents a dislocation model that accounts for the (unusual) experimentally observed behaviour. Mercuric iodide is known to be a highly anisotropic layered material, consisting of alternating layers of mercury (Hg) and iodine (I) in the stacking sequence Hg I I Hg I I . . . Bonding between two iodine layers (thought to be primarily Van der Waals) is very weak and thus slip between iodine layers (specifically, slip of (0 0 1) planes) is very easy. (Graphite is another example of such a "layered" material.) Because of its unusual bonding characteristic and resulting high anisotropy, single crystal HgI_2 provides an interesting system for studying certain fundamental deformation processes. Furthermore, the intrinsic, scientific interest in mercuric iodide's plasticity and dislocation structure (e.g. the types, mobilities, interactions, and distributions of dislocations present in the crystal) is augmented by a technological importance that attaches to this subject owing to the usefulness of the crystals as room temperature radiation detectors in low energy X-ray spectrometers [1–6]. The performance of such detectors evidently depends upon dislocation structure [7], although quantitative details have yet to be determined. A major problem in the production of HgI_2 radiation detectors is the relatively low yield of good detectors from a given crystal. Since changes in dislocation structure can be induced by deformation (e.g. from handling the crystal during detector fabrication or even from internal stresses that may occur during crystal growth), it is of practical importance to understand not only the nature of the dislocation

*This work is based upon parts of the PhD Dissertation of Timothy W. James, University of California, Santa Barbara.
†Presently at Santa Barbara Research Center, Goleta, California 93117, USA.

0022–2461/83 $03.00 + .12

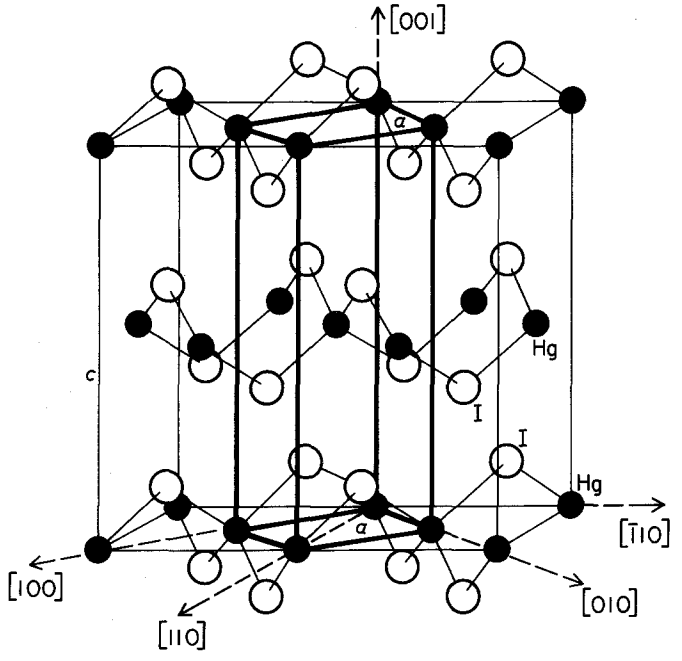

Figure 1 Tetragonal crystal structure of α-HgI_2; crystallographic axes are shown in terms of Miller indices.

structure in HgI_2 single crystals, but also the influence of stresses upon deformation and dislocation structure. Finally, single crystal HgI_2 is to be grown in zero gravity, in space, on a future NASA Space Lab mission; since the space grown crystals unavoidably will be subjected to stresses upon re-entry to earth's atmosphere, it is necessary to study the influence of stress upon the terrestrial grown crystals in order to be able to evaluate the space grown crystals properly.

Mercuric iodide's crystal structure [8, 9] in its equilibrium phase at room temperature is tetragonal, with point group 4/mm and space group $P4_2/nmc$, as illustrated in Fig. 1; this phase is often referred to as α-HgI_2 or the "red phase" (owing to its bright red colour). At 127° C, single crystal α-HgI_2 transforms to an orthorhombic form which is not of current interest as a radiation detector and does not concern us here.

As part of the current work, we carried out several types of mechanical tests, including microhardness, bending and uniaxial compression. Tensile testing was eliminated because of (i) the "softness" of the crystals (which made it difficult to grip the ends of the specimens) and (ii) the relative smallness and scarcity of HgI_2 single crystals (which made it necessary to use small test specimens). The states of stress in a "uniaxial" compression test are certainly less complex than those associated with microhardness or bending; for this reason, prominence is given here to the uniaxial compression testing. We found (in the compression tests) that, for all crystallographic orientations wherein a non-zero shear stress component acts on the (0 0 1) planes, the crystals are easily plastically deformed by slip of the (0 0 1) planes; furthermore, the (0 0 1) planes are the only planes that exhibited slip in these tests. We also found this mode of plastic deformation to exhibit work hardening (i.e. the critical resolved shear stress for slip of the (0 0 1) planes increases as plastic deformation progresses). Within the limits of accuracy and repeatability of our tests, we could not observe any anisotropy of slip direction within the (0 0 1) planes; thus, we simply speak of (0 0 1) slip, without reference to a specific slip direction parallel to the (0 0 1) plane. In cases where the shear stress on the (0 0 1) planes is zero (i.e. when the crystals are loaded either parallel or perpendicular to the [0 0 1] direction), under sufficient load, failure occurs by brittle fracture (prior to any macroscopically observed plastic deformation). In an earlier paper [10], we examined dislocation motion in HgI_2 under the influence of Knoop microhardness indentation carried out on cleaved (0 0 1) surfaces. By etching the (0 0 1) face after indentation, arrays of dislocation etch pits (emanating from the indentation) could be observed. The etch pits were square (indicating dislocations perpendicular to the cleaved (0 0 1) surface) and their edges were parallel to the ⟨1 0 0⟩ directions. The arrays

themselves were also parallel to the ⟨100⟩ directions.

From our experimental results, we induce a dislocation model, for the plastic deformation of mercuric iodide, wherein two types of dislocations play important roles. The dislocations of one type glide relatively freely in (0 0 1) planes and the movement of these dislocations gives rise to the easy slip of these planes. (Hence these dislocations are called "easy glide" dislocations). The other type of dislocations, which we call "hard glide" dislocations, are those observed in the etching of the (0 0 1) surface. These dislocations are mobile under the high, localized stress caused by a hardness indentation; however they are not sufficiently mobile to produce observable (macroscopic) plastic deformation in the compression tests. In our model, the pinning of the easy glide dislocations (as they move on (0 0 1) planes) by the hard glide dislocations (that intersect these planes) is responsible for the observed work hardening. The easy glide and hard glide dislocations thus serve, respectively, as "glissile" and "forest" dislocations during (0 0 1) slip, although the hard glide dislocations are glissile during the hardness indentations [10].

2. Bending tests

As an example of mercuric iodide's unusual mechanical properties, we mention briefly the results of a simple bending test in which a thin, single crystal, slab of HgI_2 was bent with a pair of tweezers. (The test was carried out at room temperature and at liquid nitrogen temperature, and in both cases the results were qualitatively the same.) The [0 0 1] axis was perpendicular to the "top" and "bottom" surfaces of the slab, so the slab can be thought of as comprised of layers of (0 0 1) planes (somewhat like a deck of cards, with the individual cards representing the (0 0 1) planes). The slab was gripped in the centre; the "axis" of the tweezers (and hence the bending axis) was parallel to the (0 0 1) planes; the slab was simultaneously restrained on one side and rotated with the tweezers as illustrated in Fig. 2a. If the slab were made of a ductile metal (with several active, noncoplanar slip systems), under the action of a sufficient bending moment, it would be expected to bend into the form of an "L" (as shown in Fig. 2b), with plastic deformation occurring primarily in the neighbourhood of the bend. Note, however, that this configuration would not allow the original layered structure of HgI_2 to be preserved since the plane whose trace is bb′ (or simply plane bb′) would have to become longer than plane aa′. The original layered structure could be preserved if the (0 0 1) planes were to undergo uniform slip throughout each leg of the "L", as illustrated in Fig. 2c, or if the (0 0 1) planes were to delaminate; however, neither of these behaviours occurred in the experiment. What, in fact, did occur was a spontaneous bend in the unrestrained end of the slab, as illustrated in Fig. 2d; a photograph of the bent crystal is shown as Fig. 2e. This behaviour can be explained by assuming (i) slip occurred only on the (0 0 1) planes during bending and (ii) it was energetically most favourable for slip to occur only in the central region of the slab (i.e. in the region between 1 and 2 in Fig. 2d); the spontaneous bending at 2 allows plane aa′ to remain the same length as plane bb′ as slip proceeds. (An analogous "experiment" can be performed by tightly gripping a multi-page, soft-covered book at the bound "edge" and at the "edge" opposite the binding, then bending the book about an axis parallel to the binding, while restricting slip of the pages at the bound and the opposite "edges," and preventing the pages from separating.)

In addition to the "large angle" bend test described above, carefully controlled "small angle" bend tests were carried out on single crystal HgI_2 slabs of the same orientation (as described above) using a Tinnius Olsen Tour Marshal stiffness tester. The apparatus applies a bending moment and indicates the resultant angular deflection. The specimens were held in a stainless steel clamp covered with a mylar film. A detailed description of the apparatus can be found in an operator's manual provided by the manufacturer. Briefly, the bending moment was applied by a pendulum weight arrangement against which the specimen was bent. The specimen was rotated into the pendulum by a manually operated crank. The curves of bending moment versus angular deflection were similar in appearance to the curves exhibiting plastic deformation in compression (see Fig. 6 in Section 3.3); i.e. these curves exhibited a linear elastic response in the initial stages of loading, followed by yielding and plastic deformation (which was accompanied by work hardening). This behaviour is discussed more fully in Section 3.3.

3. Compression testing

3.1. Sample preparation

Single crystal compression specimens were prepared from irregularly shaped single crystals that were vapour-grown by W. F. Schnepple and L. van den Berg at E.G. & G., Inc., Santa Barbara Operations, using the temperature oscillation crystal growth method [1, 11]. (The bending specimens discussed in the prior section were also prepared from the same crystals). Generally a number of individual compression specimens of the same orientation were produced from the "parent crystal"; crystal orientation was determined as follows. The parent crystal was mounted on a two-axis goniometer using Apiezon W wax dissolved in trichloroethylene (the wax is produced by Apiezon Products Ltd., London). Then (after waiting overnight for the wax solution to dry), the orientation of the crystallographic axes (relative to the two-axis goniometer) was determined with the aid of an optical microgoniometer (Unitron model No. GM5-181). Specifically, the orientation of the (0 0 1) plane was identified by cleaving a small piece from a corner or edge of the specimen (cleavage readily occurs parallel to the (0 0 1) plane). The exposed (0 0 1) face on the parent crystal was then chemically etched to reveal etch pits, the orientations of which were used to identify the [1 0 0] and [0 1 0] directions [10]. Next a number of single crystal compression specimens of a predetermined crystallographic orientation were fabricated from the parent crystal; fabrication was accomplished as follows. (i) A flat, "load-bearing" face (i.e. a face upon which the external load would act during compression testing) was solution machined on the parent crystal using a South Bay Technology (Temple City, California, USA) Model 460 crystal facing and polishing instrument containing an

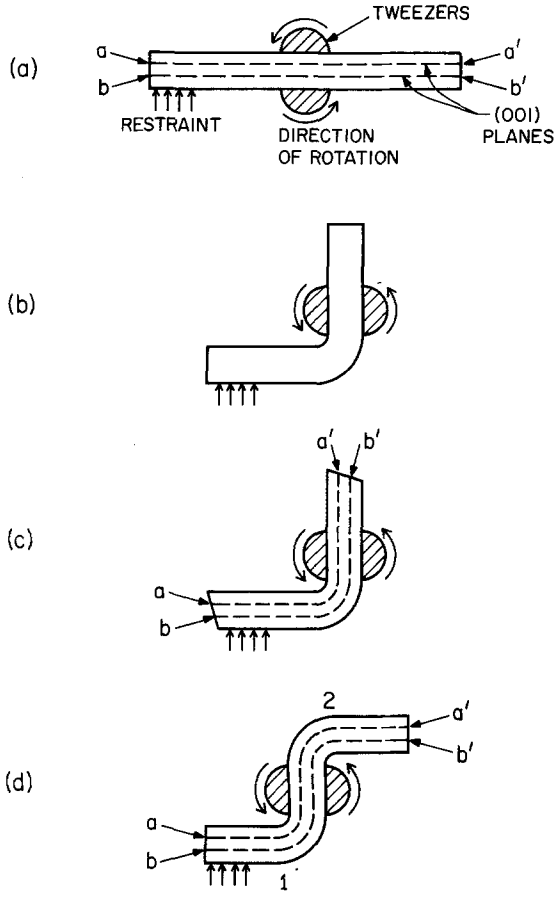

Figure 2 (a) Side view illustration of the initial stages of the bending of a single crystal slab of HgI_2. Line segments aa′ and bb′ represent the traces of two distinct (0 0 1) planes. (b) Configuration expected after sufficiently bending a ductile metal slab under the action illustrated in Fig. 2a. (c) A possible mode of bending the single crystal slab of Fig. 2a into a "modified L" wherein the bent slip planes remain equidistant and slip occurs throughout the slab; the length of plane aa′ remains equal to that of bb′. (d) Actual configuration observed in the bending of the single crystal slab of Fig. 2a. (e) Photograph of a single crystal slab of HgI_2, bent under the action illustrated in Fig. 2a.

aqueous KI solution. (ii) The crystal was removed from the goniometer by dissolving the mounting wax with TCE; it was remounted, and a second load-bearing surface was solution machined flat and parallel to the first. (iii) Finally, the crystal was "diced" (by potassium iodide solution string sawing) into a number of rectangular parallelepipid compression specimens (a typical size was 2 mm × 2 mm × 3 mm; the long axis was coincident with the loading direction). The "string sawing" was done perpendicular to the load-bearing surfaces.

3.2. Apparatus and testing techniques

The small size, chemical reactivity, and softness of the single crystal HgI_2 specimens made it necessary to design and build a specialized micromechanical uniaxial compression testing apparatus and temperature control chamber. In this apparatus, axial loads were applied vertically by placing the specimen between the faces of a moveable upper pyrolytic graphite mandrel and an essentially stationary lower mandrel, also of pyrolytic graphite. The upper mandrel was constrained by an alignment bushing so that its face remained parallel to that of the lower mandrel. Pyrolytic graphite was chosen for its inertness with HgI_2 and its large anisotropy of heat transfer coefficients. The mandrels were fabricated in such a manner that heat transfer from the specimen to the loading fixture was minimized. The top mandrel was driven by a custom made precision servo controlled mechanical testing machine. The machine could maintain controlled deflection rates to within 0.5% error over the range of 0.5 to 1000 $\mu m\,sec^{-1}$. The compression load on the specimen was measured by a strain gauge load cell attached directly to the lower graphite mandrel. Three load cells were available; their maximum load capacities were 20, 100 and 1300 N. Each load cell is compensated for off axis loading (i.e. is resistant to extraneous bending and side loading forces) and has a resolution of better than 0.05% of full scale.

In tests at elevated temperatures, the specimen and graphite mandrels were surrounded by a dry nitrogen atmosphere contained in an insulated chamber. The chamber temperature was controlled by means of a thermocouple and a resistive heating element in the nitrogen atmosphere. The specimen temperature, which was measured by a thermocouple in contact with the specimen, could be maintained to ± 2°C in the range from 20°C to the phase transformation temperature (127°C).

Specimen deformation (strain) was measured with an optical (non-contact) extensiometer (a modified Optron Model 511-S, produced by Optron, a division of Universal Technology Inc., Woodbridge, CT 06525). This technique was found to be useful because the softness of HgI_2 made it difficult to attach gauges to the specimen. Also, the use of an optical extensiometer allowed the deformation measurement equipment to be placed outside the temperature controlled chamber. (The insulated chamber was fitted with a quartz window, through which the elevated temperature optical strain measurements were made.) The extensiometer allowed the relative displacement of the specimen ends to be measured to ± 5 μm. Most of the compression tests were carried out with the upper mandrel moving at a constant rate (and thus with the crystal subjected to a fixed rate of deformation). However, in some cases, we also employed a servo-control circuit to carry out constant load creep tests at room and elevated temperatures. The control circuit consisted of an analog closed loop servo system that controls deformation rate in such a manner that the compression load is maintained constant.

3.3. Results and discussion

Over eighty compression tests were performed on single crystal, HgI_2 specimens oriented variously with respect to the loading axis. Three characteristic loading responses were observed; these depend upon crystal orientation, according to the following classification: (case a) the axis of loading is perpendicular to the [0 0 1] axis or, equivalently, parallel to $[h\,k\,0]$, where the Miller indices h and k can be arbitrary; (case b) the axis of loading is parallel to [0 0 1]; (case c) the loading axis is neither parallel nor perpendicular to [0 0 1]; these cases are illustrated in Fig. 3. Representative examples of stress–strain curves are given in Figs. 4, 5 and 6 for cases a, b and c, respectively. In cases a and b, wherein no shear stress component acts parallel to the (0 0 1) planes, failure always occurred by a brittle fracture. No distinction in behaviour was observed among the case a loadings carried out with various crystallographic axes $[h\,k\,0]$ coincident with the loading axis. In particular, the case a failures occurred by a buckling and delamination of the (0 0 1) planes; the initial fractures occurred at stresses ranging from

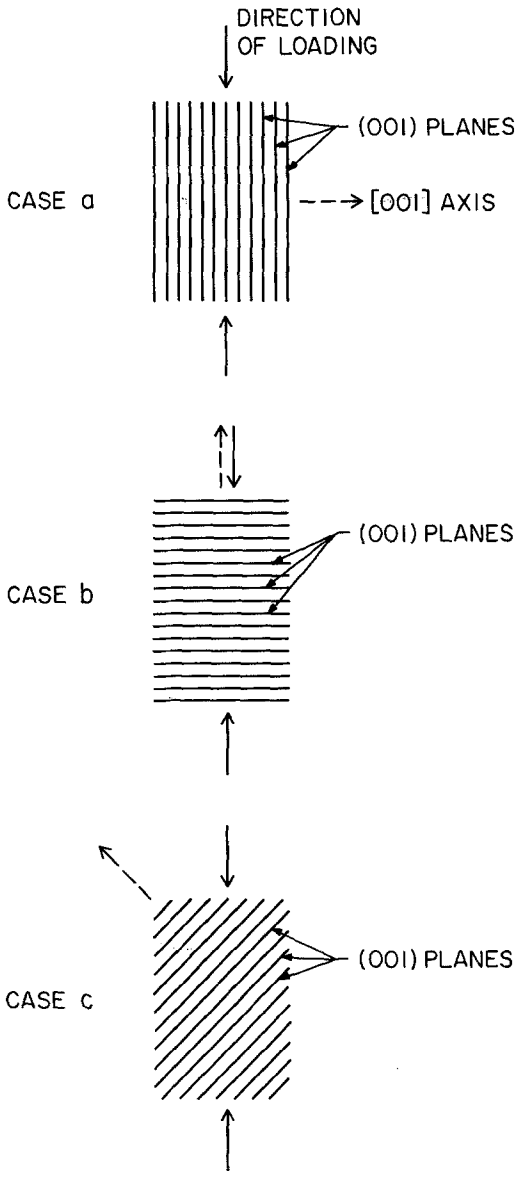

Figure 3 Illustration of the three basic crystal orientations in uniaxial compressive loading. In each case, the loading direction is vertical (indicated by solid arrows) and the [0 0 1] axis is indicated by a "dashed arrow."

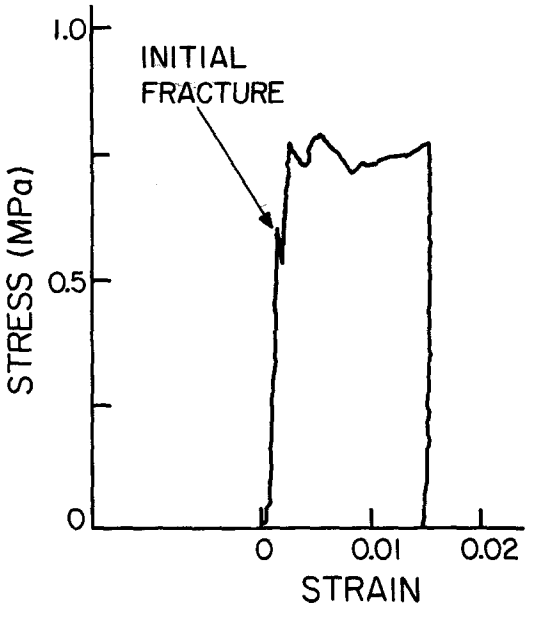

Figure 4 An example of the experimentally observed stress–strain response of HgI_2 single crystals loaded according to case a; the resolved shear stress on the (0 0 1) planes is zero.

0.4 to 1.8 MPa. For example, in Fig. 4 the sample responds in a linear, elastic manner prior to the initial fracture at about 0.6 MPa; the initial fracture is followed by a small drop in stress; then the stress increases to about 0.8 MPa and stays within the range of about 0.7 to 0.8 MPa while the specimen continues to undergo buckling and separation of the (0 0 1) planes. By contrast, in case b loadings, a region of linear, elastic response is followed by "catastrophic," brittle failure; this occurs even at temperatures close to the 127° C phase transition. The case b specimens were shattered into numerous small fragments; these fragments contained both jagged and flat, smooth, fracture surfaces. The flat, smooth, fracture surfaces corresponded approximately with planes of maximum shear stress, i.e. the normals to these surfaces were at about 45° to the loading axis. Also, these fracture surfaces characteristically intersected the (0 0 1) face in ⟨1 0 0⟩ directions and were similar in appearance to the surfaces produced by cleavage of the (0 0 1) planes, thus suggesting the presence of secondary cleavage planes.

The case b loadings were capable of supporting the greatest axial loads; the average fracture stress was about 32 MPa, although fracture stresses as low as 5.0 MPa (at 112° C) and as high as 81.4 MPa (at 24° C) were observed. (The variations in case b fracture stresses, among different samples at the same temperature, were comparable to the variations observed among tests at different temperatures, so no conclusions are drawn concerning the temperature dependence of the case b fracture stress.) The large ranges of fracture stresses observed in cases a and b were not unexpected since large variations in fracture stress are characteristic of brittle failures in general. The fact that the fracture stress in case a is much lower than in case b

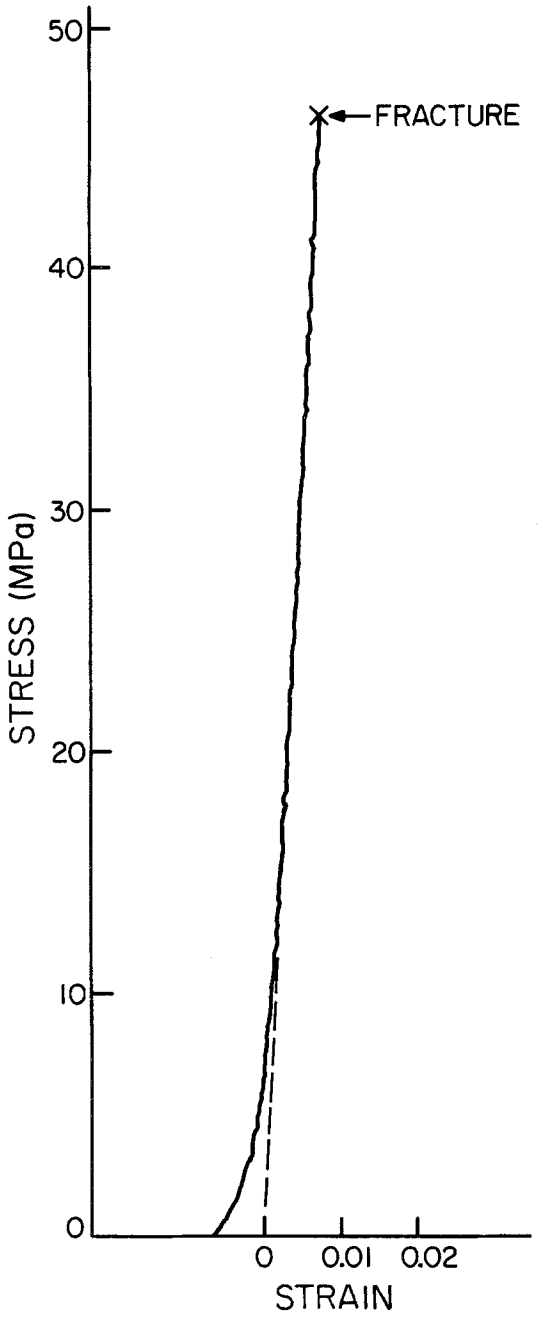

Figure 5 An example of experimental stress–strain behaviour of HgI_2 single crystals subjected to case b loading; the resolved shear stress on the (0 0 1) planes is zero. The initial upward curvature of the stress–strain curve is evidently an "instrumental effect," resulting from a slight "crown" in the specimen's load bearing faces, and is not a material property. This effect can also be observed in Figs. 4 and 6, although to a lesser extent.

is readily understood in terms of the weak bonding between the (0 0 1) planes (which evidently begin to separate upon failure in case a).

Throughout the manifold of compression tests of types a and b, each crystallographic plane $(h\,k\,l)$ was subjected to non zero (resolved) shear stresses in all directions within that plane, with the exceptions of (i) the (0 0 1) plane in the $[h\,k\,0]$ directions (i.e. in all directions parallel to (0 0 1)) and (ii) planes of the type $(h\,k\,0)$ in their [0 0 1] direction. The absence of observed deformation by slip in these tests leads us to preclude the existence of glissile dislocations in our specimens on all crystallographic planes, with the possible exceptions of (0 0 1) and $(h\,k\,0)$, i.e. with the possible exceptions of planes perpendicular and parallel to the [0 0 1] axis; glissile dislocations on planes $(h\,k\,0)$ would have Burgers vectors parallel to the [0 0 1] direction. The actual existence of glissile dislocations on (0 0 1) planes is induced from the results of the case c loadings, discussed in the following paragraphs; these dislocations are readily moved and are termed easy glide dislocations. The existence of glissile dislocations on planes of the $(h\,k\,0)$ type was demonstrated by the etch pits produced after hardness indentation of (0 0 1) surfaces, as we reported earlier [10]. Specifically, the indentation-etch pit study showed these dislocations to lie and to propagate on the {1 0 0} planes; the direction of propagation indicated by the etch pits was ⟨1 0 0⟩. Thus, we can further presume that these are screw dislocations, at least at their termini on (0 0 1) faces. Quite possibly, individual pairs of screw dislocation segments on {1 0 0} are linked (within the crystal) by edge dislocation segments, thus forming dislocation half-loops or segments of loops that are terminated on the (0 0 1) face where the screw dislocation segments meet the (0 0 1) face. The dislocations on the {1 0 0} planes are relatively immobile; i.e. although these dislocations moved under the high, localized stresses generated by the hardness indentations (of [10]), they did not move sufficiently to produce observable slip of {1 0 0} planes during the case c loadings (which are reported here); thus, these are termed hard glide dislocations. (We realize, of course, that in principle, it may be possible to generate and/or move glissile dislocations on other planes $(h\,k\,l)$ under stresses that are higher than those reached in the present tests. However, such dislocations, if indeed they were to exist, evidently do not play a role in the plastic deformation processes of present concern and are not important to this discussion.) We

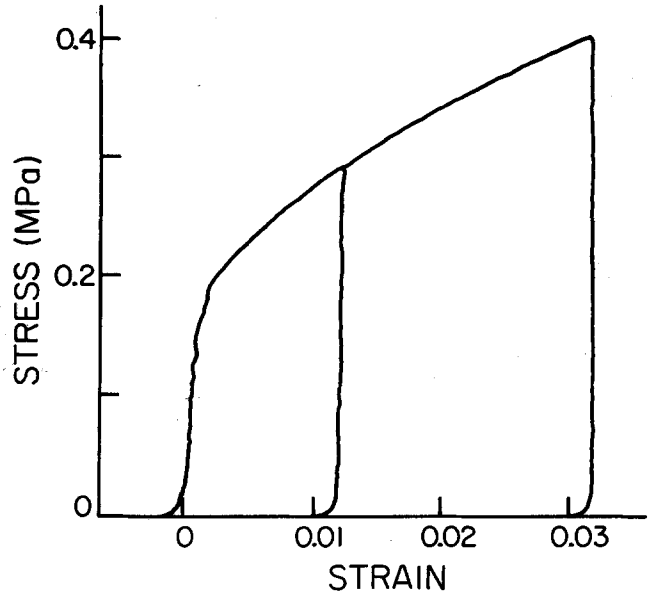

Figure 6 An example of the stress–strain response of HgI_2 single crystals loaded as in case c. (Here the compression axis was coincident with the (0 1 1) plane and was at 45° to the [0 0 1] direction, although the response is characteristic of all case c loadings, regardless of crystal orientation within the case c classification.)

note also that the above conclusions regarding dislocation structure are consistent with the results of the large angle bending test discussed in Section 2; i.e. in that test, observable slip occurred on (0 0 1) planes only.

Case c loadings were carried out for a variety of orientations of the [0 0 1] axis with respect to the loading direction. The three salient features of the case c responses are (i) the crystals exhibit plastic deformation by slip of the (0 0 1) planes, (ii) the crystals work harden while undergoing plastic deformation by (0 0 1) slip, and (iii) the stress–strain curves of "as-grown" crystals (i.e. crystals not subjected to prior work hardening) exhibited linear, elastic behaviour up to critical resolved yield stresses of about 0.1 MPa. A typical example is shown in Fig. 6; here the sample initially responds in a linear, elastic manner up to an applied stress of 0.16 MPa (in this case, the [0 0 1] axis was at 45° to the axis of compression, so the maximum resolved shear stress on the (0 0 1) planes is one-half the applied stress). At 0.16 MPa applied stress, the sample begins to yield by slip of the (0 0 1) planes. Plastic deformation by (0 0 1) slip progresses while the strain is increased continuously to about 0.012 (where the corresponding stress is 0.29 MPa). Then the load is continuously reduced to zero (during which the crystal responds in a linear, elastic manner). Upon reloading, the crystal response is also linear, elastic (without evident hysteresis) up to about 0.29 MPa (i.e. up to the "yield stress" to which the crystal has work hardened in the initial loading); the crystal then plastically deforms to a strain of 0.032 and stress of 0.4, after which the load is removed, leaving the crystal with a "permanent" strain of about 3%.

The easy (0 0 1) slip and the work hardening found in the case c loadings (when considered in conjunction with the results of the case a and b loadings (discussed above) and microhardness indentations [10]) led us to conclude that the (0 0 1) slip occurs by the movement of "easy glide" dislocations, the cores of which are parallel to the (0 0 1) planes, and that the work hardening is a result of the interaction of these easy glide dislocations with the "hard glide" dislocations observed earlier [10]. (This model for plastic deformation was first presented in T. W. James' PhD Dissertation, University of California, Santa Barbara, 1980.) Recently, Gits and Authier [12] studied these easy glide dislocations by means of X-ray topography, and identified their Burgers vector to be [1 0 0] and [1 1 0]. These dislocations have heretofore escaped observation by direct etching-optical microscopy techniques. The difficulty of producing and observing etch pits from the dislocations on the (0 0 1) planes is no doubt a result of the very weak bonding between successive iodine layers on these planes; etches tried to date have evidently been either too destructive or too inert to produce the desired result.

Information about the influence of temperature upon the interaction between the easy and hard glide dislocations can be obtained from creep and annealing experiments. Examples of results of

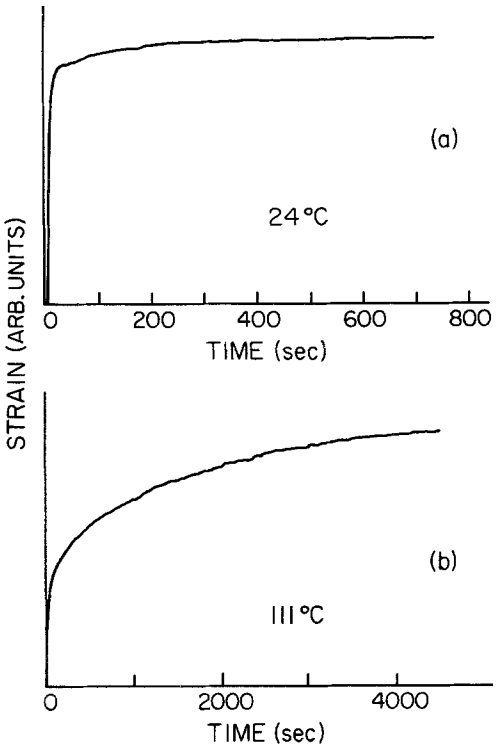

Figure 7 Examples of constant load, creep tests at room and elevated temperatures for case c compressive loadings (crystal orientation here was also as is described in the caption for Fig. 6).

constant load creep tests are given in Figs. 7a and b. Constant loads, sufficient to cause considerable plastic deformation and work hardening, were rapidly applied at time zero. The loads in Figs. 7a and b were set in such a manner that, upon application of the load, the compressive stresses were the same in both tests (i.e. the initial stresses were identical). In each case, a substantial, almost instantaneous strain occurs upon application of the load; this strain is mainly plastic (i.e. it does not contain but a very small elastic component). Following the initial response, significant differences appear in the creep behaviour at the lower and higher temperatures; at the lower temperature, the creep rate rapidly approaches zero, whereas, at the higher temperature, the creep rate decays much more gradually (note the difference in time scales in Figs. 7a and b). In terms of the dislocation model, at low temperatures, the hard glide dislocations provide an effective barrier to the motion of the easy glide dislocations, and hence the creep rate rapidly approaches zero. At higher temperatures, thermal activation enables greater creep to proceed; two possible mechanisms are 1. an increased mobility of the hard glide dislocations at higher temperatures and/or 2. an increased ability of the easy glide dislocations to become unpinned from the hard glides as temperature increases. In the case of mechanism 1, the easy glide dislocations would more easily "drag" the hard glides, thus allowing creep to proceed. Proof that the hard glide dislocations do indeed become more mobile as temperature increases was found by Milstein *et al.* [13] in their microhardness tests carried out at elevated temperatures.

Constant load "creep" tests were also performed with the loading axis perpendicular to the (0 0 1) planes. In these tests, the samples exhibited only a linear, elastic response (i.e. no plastic deformation), at both room and elevated temperature, as expected (i.e. neither the easy glide nor the hard glide dislocations are subjected to a resolved shear stress, as discussed earlier).

Thermal annealing tests also gave results that were consistent with the dislocation model and with the increased mobility of the hard glide dislocations at higher temperatures. Compression specimens of the case c configuration were work hardened at 20° C to permanent strains in the range of 0.034 to 0.21 and their expected yield stresses (i.e. the stresses to which they were work hardened) were recorded. The specimens were then sealed in a glass ampoule (back filled with argon) and annealed at 115° C for 24 h. After the anneal, the specimens were again compressed at 20° C and their initial yield stresses were recorded. Additional samples were work hardened in compression at 20° C, then annealed at 20° C for periods of at least 24 h (under zero applied load), and finally retested in compression to determine the change in expected yield stress in the absence of the elevated temperature anneal. In cases of large plastic deformation (i.e. plastic strains of about 0.2), very small (but measurable) reductions in expected yield stress occurred after a 20° C anneal, while substantial (in the range of 20 to 30%) reductions occurred after the 115° C anneal. For plastic strains of about 0.03, neither the room temperature nor the 115° C anneals caused a detectable reduction in expected yield stress. Evidently, for the large plastic strains (of the order of 0.2), the forces of interaction (between sufficient numbers of easy and hard glide dislocations) are large enough so that the increased thermal agitation during the 115° C anneals causes the easy glide dislocations to become unpinned

more readily from the hard glide dislocations and/or the hard glide dislocations (whose mobility increases with increasing temperature [13]) are moved sufficiently to cause a reduction in yield stress during the 115° C anneals. For the large plastic strains and room temperature anneals, while presumably there exist large interaction (pinning) forces between large numbers of easy and hard glide dislocations, the lack of sufficient thermal agitation and/or mobility of the hard glide dislocations precludes significant reduction of yield strength during anneal. In the case of small plastic deformations, pinning forces between dislocations evidently are insufficient to cause appreciable movement of the hard glides or unpinning of the easy glides, even at 115° C.

In summary, we have performed numerous and various mechanical deformation tests on single crystals of α-HgI_2 and have formulated a dislocation structure model that is consistent with the experimental results. The essential features of the model are as follows. (i) There exist easily moved dislocations or dislocation segments, the cores of which are parallel to the (0 0 1) crystallographic planes; these are termed "easy glide" dislocations. (ii) Although the easy glide dislocations can move readily on (0 0 1) planes, individual easy glide dislocations do not climb out of their (0 0 1) slip planes. (iii) There exist relatively immobile dislocations or dislocation segments ("hard glide" dislocations) that intersect the (0 0 1) planes. The cores of the hard glide dislocations are parallel to the {1 0 0} planes. These dislocations are relatively immobile in the sense that a large resolved shear stress is required in order to move them. Their mobility increases with increasing temperature. (iv) The two types of dislocations (i.e. the "easy" and "hard" glide) are the only dislocations that contribute to plastic deformation; however, under almost all modes of loading, plastic deformation occurs by slip of the easy glide dislocations. (v) When the easy glide dislocations move on the (0 0 1) planes, they interact with the hard glide dislocations. The interaction interferes with the movement of (or "pins") the easy glide dislocations, thus causing work hardening.

Acknowledgements

The authors are very grateful to E. G. and G., Inc., Santa Barbara Operations, Goleta, CA, for supplying the single crystals used in the present study and for a research grant that supported this work. We wish to express particular appreciation to Mr. W. Schnepple, Dr L. van den Berg, Dr M. Schieber and Mrs C. Ortale for many helpful discussions and invaluable assistance.

References

1. M. SCHIEBER, W. F. SCHNEPPLE, and L. van den BERG, *J. Crystal. Growth* **33** (1976) 125.
2. M. SCHIEBER, *Nucl. Inst. Methods* **144** (1977) 469.
3. A. J. DABROWSKI, G. C. HUTH and M. SINGH, *Appl. Phys. Lett.* **33** (1978) 211.
4. G. C. HUTH, A. J. DABROWSKI, M. SINGH, T. E. ECONOMOU and A. L. TURKEVICH, in "Advances in X-Ray Analysis", Vol. 22, edited by G. J. McCarthy, C. S. Barrett, D. E. Leyden, J. B. Newkirk and C. S. Rudh (Plenum Press, New York, 1979) p. 461.
5. R. C. WHITED and M. M. SCHIEBER, *Nucl. Inst. Method* **162** (1979) 113.
6. Proceedings of the 1982 International Workshop on HgI_2, Jerusalem, June 1982, to be published as a special issue of *Nuclear Instruments and Methods.*
7. P. T. RANDTKE and C. ORTALE, *IEEE Trans. Nuc. Sci.* **NS-24** (1977) 129.
8. G. A. JEFFREY and M. VLASSE, *Inorganic Chem.* 6 (1967) 396.
9. R. W. G. WYCOFF, in "Crystal Structures," 2nd Edition, Vol. 1(Interscience, New York, 1963) pp. 309–310.
10. T. W. JAMES and F. MILSTEIN, *J. Mater. Sci.* **16** (1981) 1167.
11. H. SCHOLZ, *Akta Electronica* **17** (1974) 69.
12. S. GITZ and A. AUTHIER, *J. Crystal Growth* **58** (1982) 473.
13. F. MILSTEIN, B. FARBER, K. KIM, L. van den BERG and W. SCHNEPPLE, to be published in *Nuclear Instruments and Methods.*

Received 15 February
and accepted 7 March 1983